Supporting Information

Frequency Stable Dielectric Constant with Reduced Dielectric Loss of One-Dimensional ZnO-ZnS Heterostructure

Amina Zafar[a,b], Muhammad Younas[c], Syeda Arooj Fatima[d], Lizhi Qian[e], Yanguo Liu[e], Hongyu Sun[e], Rubina Shaheen[d], Amjad Nisar[a], Shafqat Karim[a], Muhammad Nadeem[c], Mashkoor Ahmad[a*]

[a]Nanomaterials Research Group, Physics Division, PINSTECH, Islamabad 44000, Pakistan.

[b]Central Analytical Facility Division, PINSTECH, Islamabad 44000, Pakistan.

[c]Polymer Composite Group, Physics Division, PINSTECH, Islamabad 44000, Pakistan.

[d]Central Diagnostic Laboratory, Physics Division, PINSTECH, Islamabad 44000, Pakistan.

[e]School of Resources and Materials, Northeastern University at Qinhuangdao, Qinhuangdao 066004, P.R China.
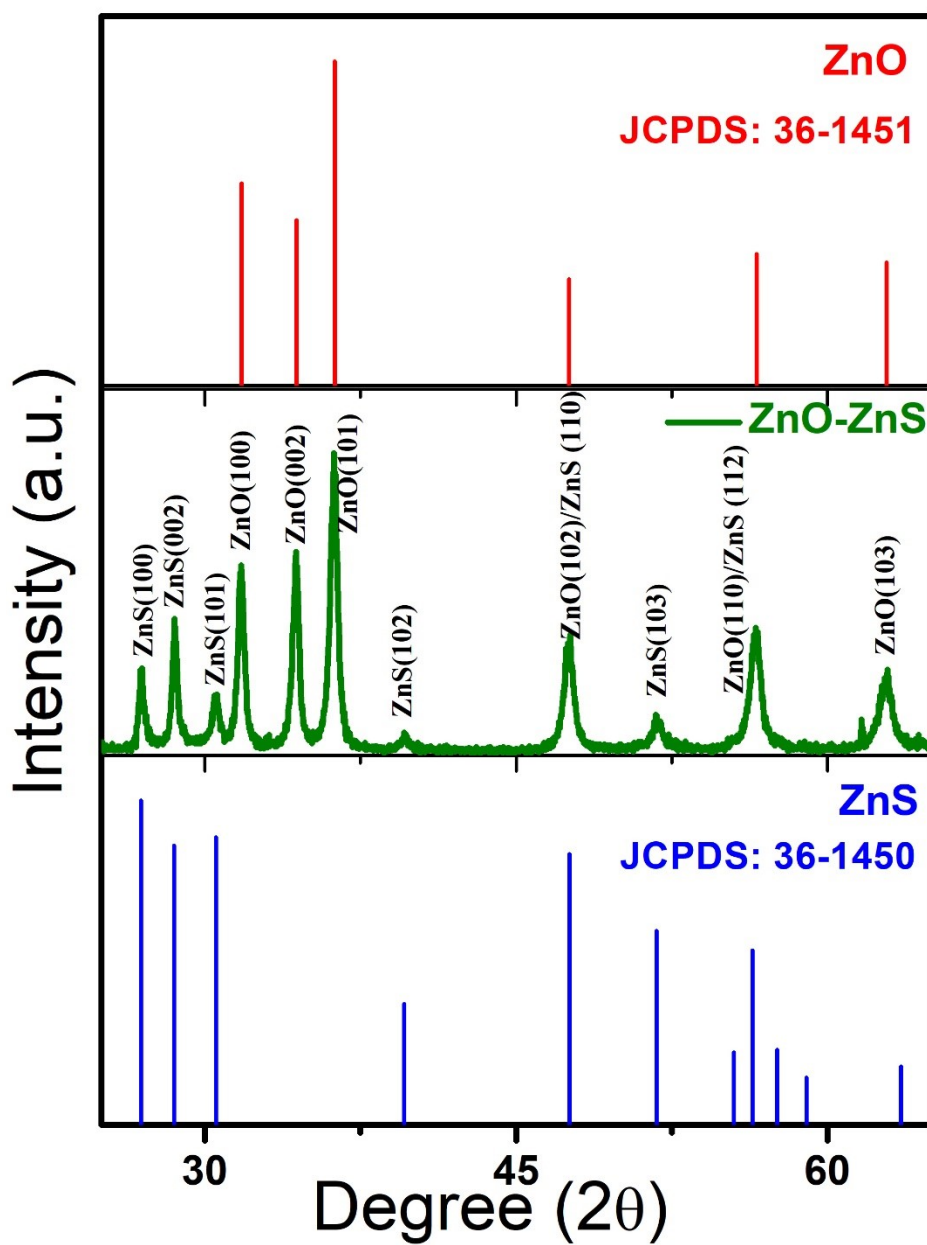
Correspondence to:mashkoorahmad2003@yahoo.com

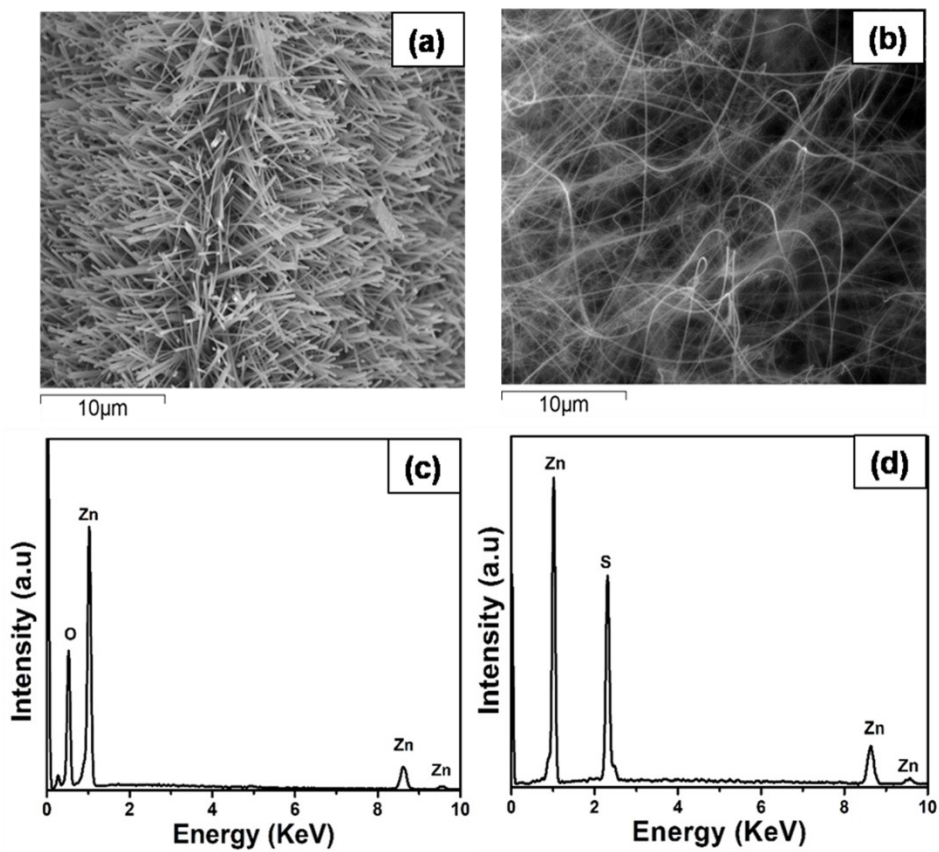**Figure S1.** XRD pattern of synthesized ZnO-ZnS heterostructure.

Figure S2. FESEM images of (a) ZnO nanorods and (b) ZnS nanowires. Corresponding EDS spectrum of (c) ZnO nanorods and (d) ZnS nanowires.
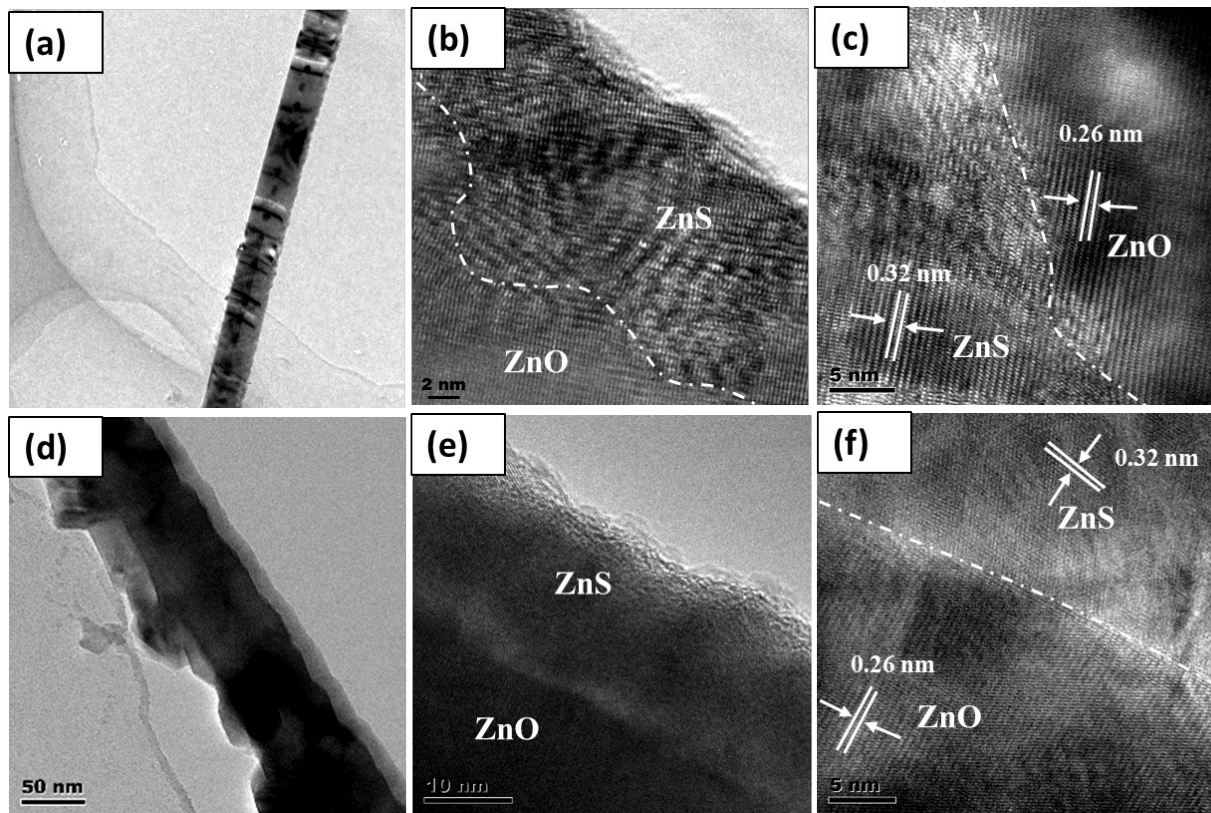
Figure S3. (a, d) Low magnification TEM images of ZnO-ZnS heterostructure and (b, c, e, f) corresponding HRTEM images from different areas.
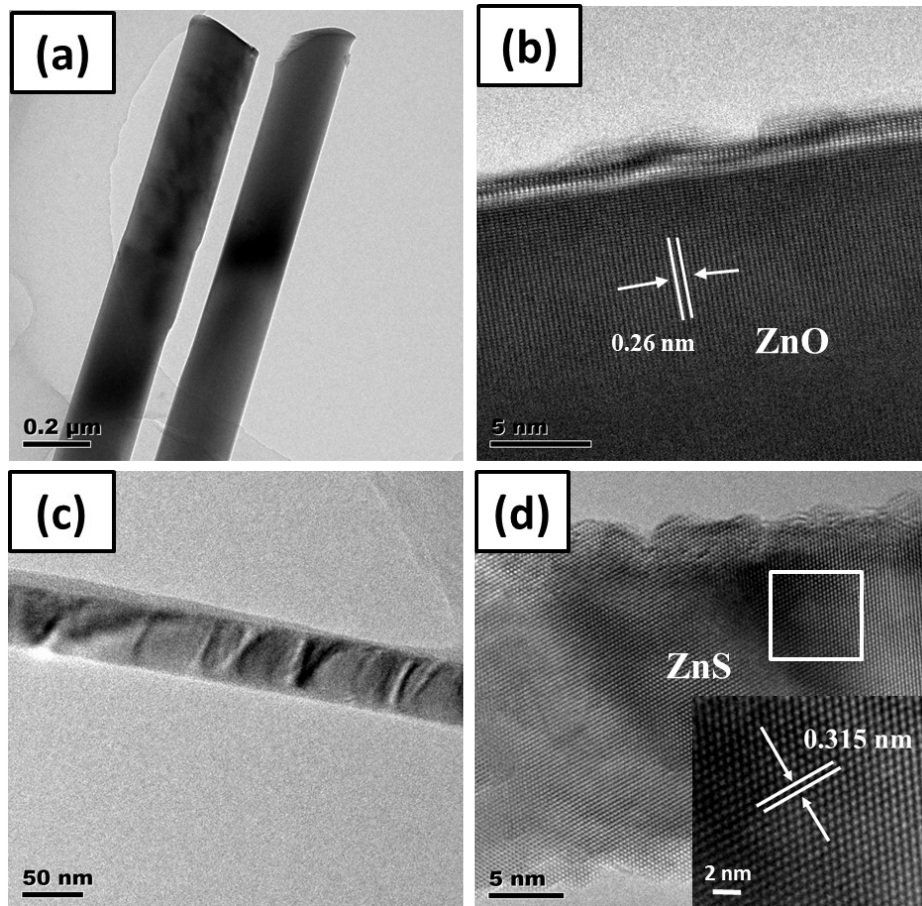
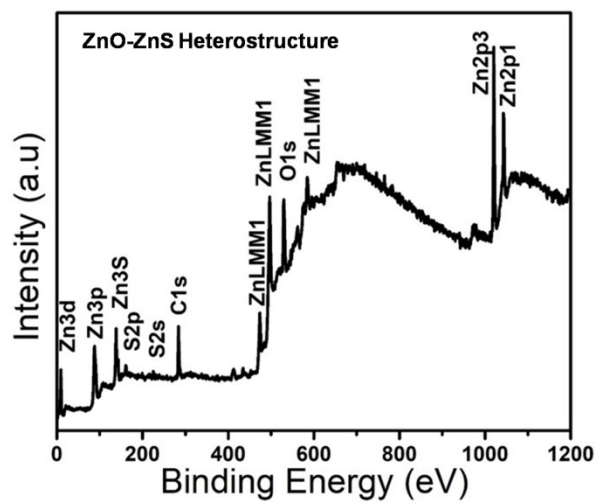**Figure S4.** Low and high magnification TEM images of (a, b) ZnO nanorod and (c, d) ZnS nanowire

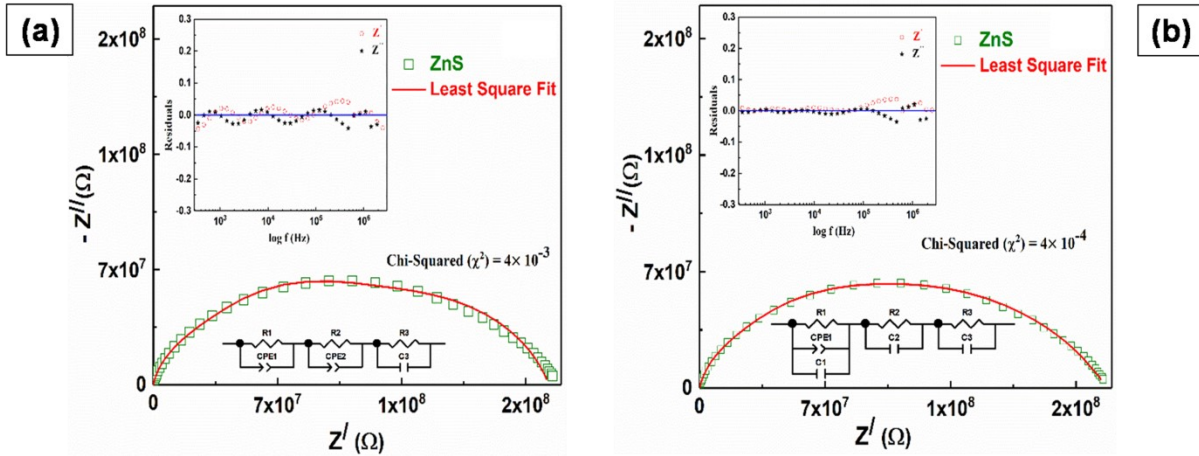**Figure S5.** XPS survey spectrum of ZnO-ZnS heterostructure.

Figure S6. Complex impedance plane plots (Z" vs. Z') of ZnS nanowires fitted with: (a) conventional equivalent circuit model and (b) bulk equivalent circuit model. The symbols and solid lines represent the data points and fitted lines, respectively. Upper left inset in each figure shows residuals between experimental and fitted data for the same sample.

Figure S7. Complex impedance plane plots (Z" vs. Z') of ZnO nanorods fitted with: (a) conventional equivalent circuit model and (b) bulk equivalent circuit model. The symbols and solid lines represent the data points and fitted lines, respectively. Upper left inset in each figure shows residuals between experimental and fitted data for the same sample.
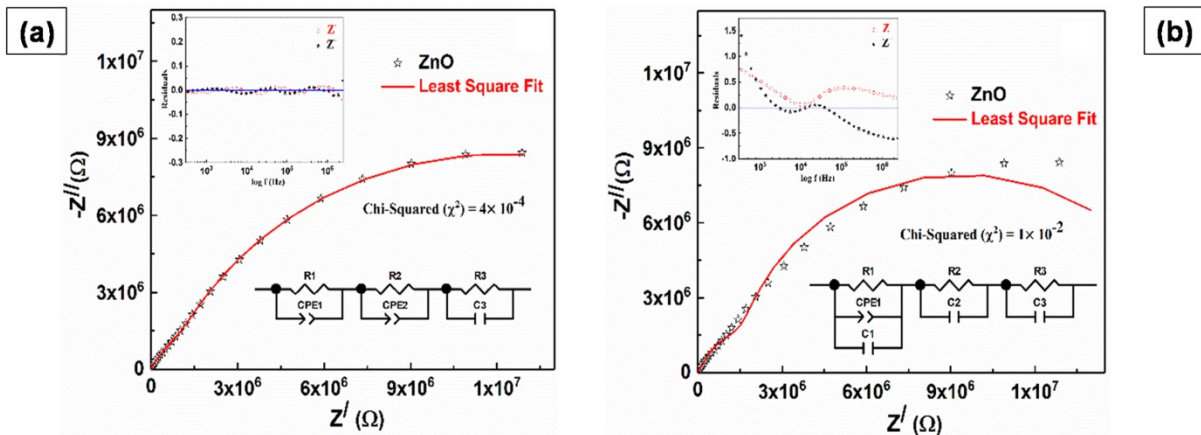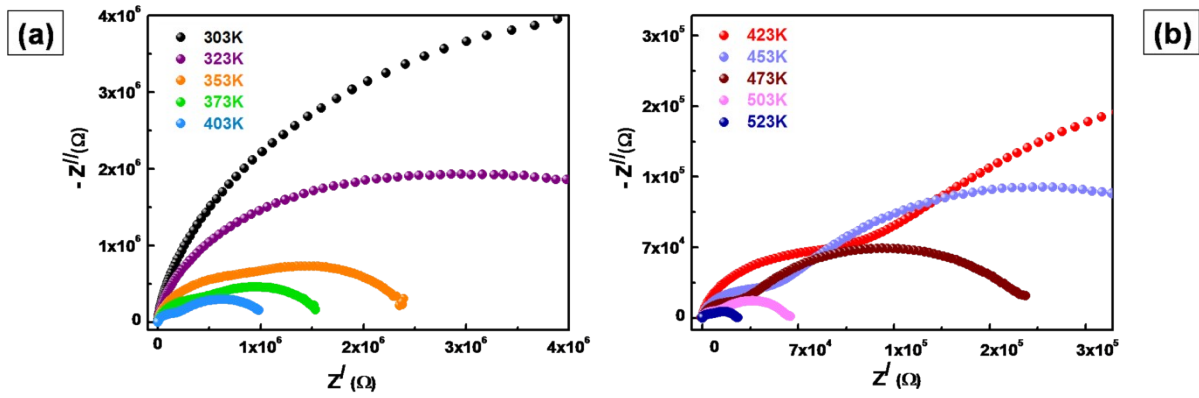
Figure S8. Complex impedance plane plots ((Z" vs. Z') for ZnO-ZnS heterostructure at various temperatures (a) 303-403 K and (b) 423-523 K.

Fitting Parameters	303K	323K	353K	373K	403K	423K	523K
R_1 (Ω)	1.422×10^6	2.2951×10^6	1.1125×10^6	557150	241750	157630	1970
R_2 (Ω)	5.679×10^6	2.4987×10^6	870130	625680	526760	429570	19086
R_3 (Ω)	4.041×10^6	1.1651×10^6	797290	412150	169810	113400	5080
C_1 (F)	2.983×10^{-11}	2.109×10^{-11}	1.991×10^{-11}	1.980×10^{-11}	1.993×10^{-11}	2.038×10^{-11}	8.511×10^{-11}
C_{11} (F)	5.517×10^{-11}	1.720×10^{-11}	1.380×10^{-11}	1.320×10^{-11}	1.280×10^{-11}	1.400×10^{-11}	1.885×10^{-11}
C_2 (F)	5.352×10^{-11}	3.193×10^{-10}	1.852×10^{-9}	1.084×10^{-9}	1.003×10^{-9}	1.196×10^{-9}	2.605×10^{-9}
C_3 (F)	1.550×10^{-10}	1.338×10^{-10}	$3.379 \text{ x} 10^{-10}$	4.00×10^{-10}	5.912×10^{-10}	7.959×10^{-10}	4.472×10^{-10}
n_1	0.711	0.690	0.670	0.660	0.614	0.538	0.500
Chi-Squared (χ^2)	5.0×10^{-5}	3.9×10^{-5}	2.1×10^{-5}	2.2×10^{-5}	6.6×10^{-5}	1.2×10^{-4}	7.50×10^{-5}
Sum of Squares	0.012	0.009	0.005	0.005	0.015	0.028	0.017

Table S1. Electrical parameters acquired from fitting of the measured data to the best fitted
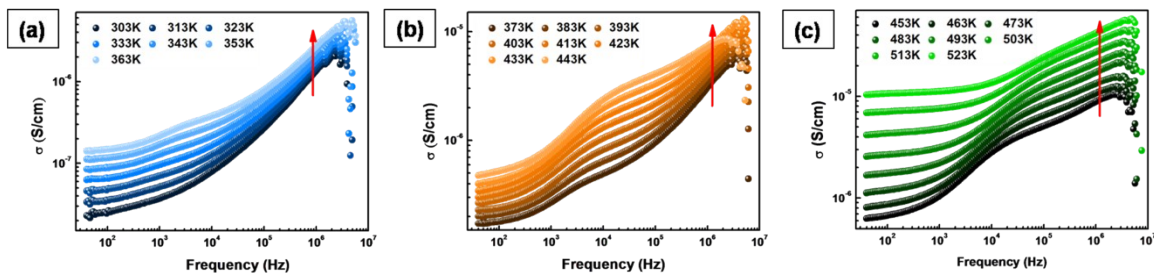
Equivalent circuit model at different temperatures.

Figure S9. (a-c) Effect of frequency and temperature on AC conductivity of ZnO-ZnS heterostructure at different temperatures.
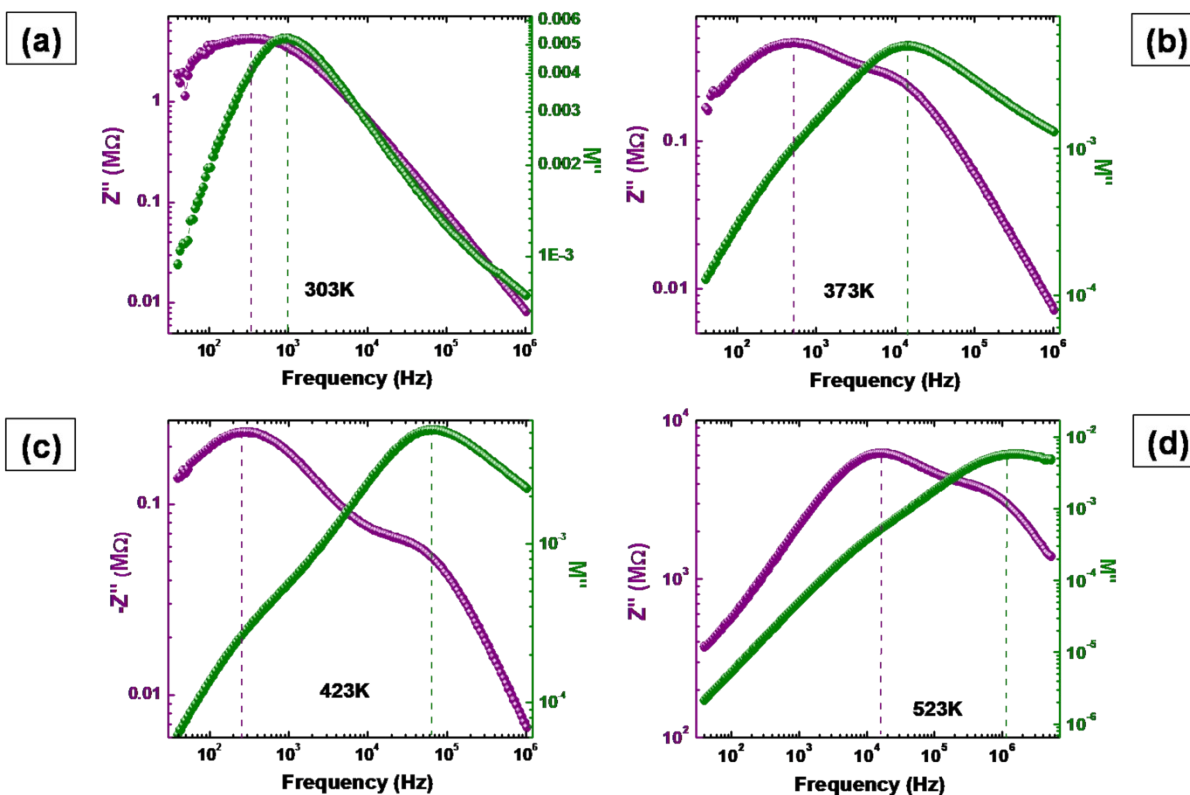

Figure S10. log-log plots of Z″ and M″ vs. frequency at different temperatures (a) 303K (b) 373K (c) 423K (d) 523K for ZnO-ZnS heterostructure.
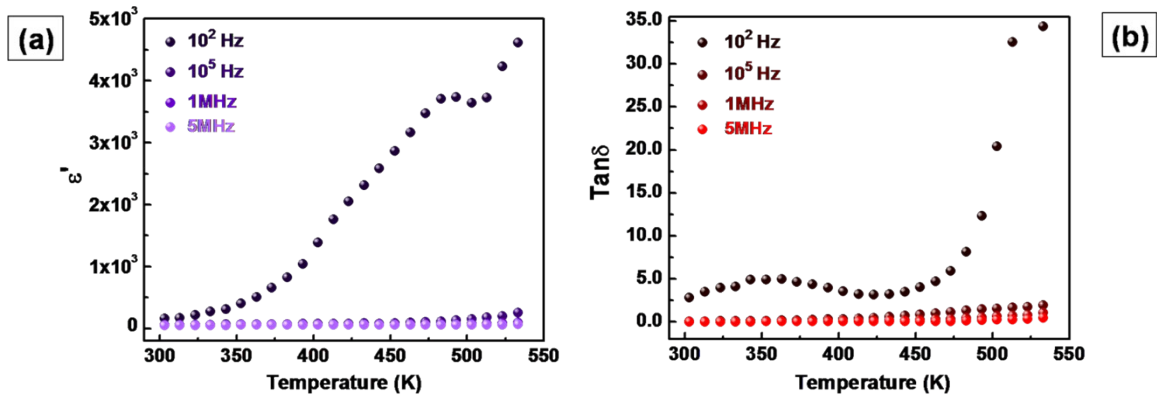
Figure S11. (a) Dielectric constant (ε') vs. temperature and (b) Tangent loss (Tanδ) vs. temperature at selected frequencies for ZnO-ZnS heterostructure.

Material	Dielectric Constant (ε')	Dielectric Loss (Tanδ)	Ref
ZnO-ZnS nanocomposites	0.75	0.09	[1]
$Zn_{0.95}Tm_{0.05}O$	75	0.12	[2]
$BaTiO_3$/P(VDF-HFP) composites (15 vol % 4L)	21	0.2	[3]
BNT@Dopa/PVDF nanocomposites	12	0.16	[4]
Ag@TiO_2/PTFE composites containing			[5]
50% vol rutile Ag@TiO_2	30	0.07	
50% vol anatase Ag@TiO_2	13	0.05	
$BiFeO_3$/PMMA nanocomposite	5.5	0.03	[6]
CeO_2/polystyrene nanocomposite (PS/20 vol % 100 nm hydroxylated CeO_2)	8.2	0.04	[7]
Grain oriented TiO_2			[8]
TiO_2-mixed (3.99 nm)	25	0.38	
TiO_2-small (3.66 nm)	65	0.9	
TiO_2-large (4.07 nm)	30	1.5	
$Zn_{1-x}Sm_xO$ nanoparticles $0.00 \leq x \leq 0.10$	~8	~0.23	[9]
N-doped ZnO (4 wt% N)	3	<0.05	[10]
B-doped ZnO (4 wt% B)	1	<0.05	
Pb doped ZnS	20-70	0.1-1.5	[11]
Cr doped ZnS	1.5-2	~0.1	[12]
ZnO-ZnS heterostructure	**57**	**0.04**	**This work**

Table S2. Comparison of dielectric constant and dielectric loss of ZnO-ZnS heterostructure with reported materials at 1MHz

References

[1] M. Sundararajan, P. Sakthivel, A.C. Fernandez, J. Alloys Compd. 2018, 768, 553.

[2] A. Bandyopadhyay, N. Bhakta, S. Sutradhar, B.J. Sarkar, A.K. Deb, S. Kobayashi, K. Yoshimura, P.K. Chakrabarti, RSC Adv. 2016, 6, 101818.

[3] L. Sun, Z. Shi, L. Liang, S. Wei, H. Wang, D. Dastan, K. Sun, R. Fan, J. Mater. Chem. C. 2020, 8, 10257.

[4] J. Li, G. Chen, X. Lin, S. Huang, X. Cheng, J. Mater. Sci. 2020, 55, 2503.

[5] F. Liang, L. Zhang, W.Z. Lu, Q.X. Wan, G.F. Fan, Appl. Phys. Lett. 2016, 108, 072902.

[6] A. Ahlawat, S. Satapathy, S. Bhartiya, M.K. Singh, R.J. Choudhary, P.K. Gupta, Appl. Phys. Lett. 2014, 104, 042902.

[7] L. Zhang, S. Chen, S. Yuan, D. Wang, P.H. Hu, Z.M. Dang, Appl. Phys. Lett. 2014, 105, 052905.

[8] G. Wang, C. Wang, J. Zheng, S. Wang, R. Ahmed, J. Sun, J. Wang, Y. Guo, J. Mater. Sci. 2020, 55, 3940.

[9] K. Badreddine, A. Srour, R. Awad, A.I. Abou-Aly, Mater. Res. Express. 2020, 7, 025016.

[10]   A.C. Güler, B. Dindar, H. Örücü, Mater. Res. Express. 2019, 6, 065017.

[11]   A. Hastir, S. Sharma, R.C. Singh, Appl. Surf. Sci. 2016, 372, 57.

[12]   J. Kumar, R. Thangaraj, S. Sharma, R.C. Singh, Appl. Surf. Sci. 2017, 416, 296.